

DOI: <https://doi.org/10.24425/amm.2023.141485>JEONG-HAN LEE<sup>1</sup>, JAE-CHEOL PARK<sup>1</sup>, HYUN-KUK PARK<sup>1\*</sup>**PROPERTIES OF TiC-Mo<sub>2</sub>C-WC-Ni CERMETS BY A HIGH-ENERGY BALL MILLING/SPARK PLASMA SINTERING**

A TiC-Mo<sub>2</sub>C-WC-Ni alloy cermet was fabricated by high-energy ball milling (HEBM) and consolidation through spark plasma sintering. The TiC-based powders were synthesized with different milling times (6, 12, 24, and 48 h) and subsequently consolidated by rapid sintering at 1300°C and a load of 60 MPa. An increase in the HEBM time led to improved sinterability as there was a sufficient driving force between the particles during densification. Core-rim structures such as (Ti, W)C and (Ti, Mo)C (rim) were formed by Ostwald ripening while inhibiting the coarsening of the TiC (core) grains. The TiC grains became refined (2.57 to 0.47 μm), with evenly distributed rims. This led to improved fracture toughness (11.1 to 14.8 MPa·m<sup>1/2</sup>) owing to crack deflection, and the crack propagation resistance was enhanced by mitigating intergranular fractures around the TiC core.

*Keywords:* TiC-based cermet; core-rim structure; high-energy ball-milling; spark plasma sintering; microstructure

**1. Introduction**

Titanium carbide (TiC)-based cermets, which are widely used in high-temperature and high-speed cutting, have a superior surface finish and higher feed rate compared to those of tungsten carbide [1]. However, it is difficult to sinter TiC due to its inherent brittleness and high melting point despite its excellent mechanical properties at ultrahigh temperatures. To compensate for these disadvantages, a sintering aid and secondary carbide may be added to TiC to improve its sinterability and fracture toughness. Ni, Co, or Fe is mainly used as the binder; particularly, Ni exhibits the best wettability toward TiC among the group 4 elements (FCC metals), thereby significantly improving its sinterability [2]. The mechanical properties of TiC are improved by transition metal carbides such as those of tungsten and molybdenum, which act as inhibitors of grain growth, forming a secondary mixed carbide phase with a cubic structure ((Ti, M)C<sub>x</sub>, M: W, and Mo). Previous studies have reported that most TiC-based cermets have a typical core-rim structure, where the core is composed of TiC and outer/inner rims of (Ti, M)C<sub>x</sub> are formed during solid-state sintering [3]. However, an appropriate compositional design is essential because concentrated Mo<sub>2</sub>C and WC can cause a decrease in the hardness and strength of TiC-based cermets by increasing the rim thickness.

A novel sintering method that can refine the particle size of the initial powder or achieve complete densification in a short

time is considered for decreasing the rim thickness, which can improve the fracture toughness of TiC-based cermets. Most conventional sintering methods, such as hot pressing, hot isostatic pressing, and pressureless sintering, result in non-uniform internal/external properties owing to the use of indirect heating systems. Therefore, the wear resistance decreases owing to grain coarsening during prolonged consolidation.

In this study, Mo<sub>2</sub>C, WC, and Ni were added to improve the mechanical properties of the TiC-based cermet materials synthesised through a high-energy ball milling (HEBM) process. The spark plasma sintering (SPS) process was applied following several repetitions of milling for an alloyed powder, and guidelines on optimising the high-density solid-state sintering process for the core-rim transformation were established. The structural evolution, sintering behaviour, microstructure, and mechanical properties of the TiC-based cermets were investigated based on the effect of the core-rim structure formation.

**2. Experimental**

TiC (≤5.0 μm, >99.9%, Kojundo Chemical Laboratory Ltd.), Mo<sub>2</sub>C (≤44.0 μm, >99.5%, Alfa Aesar), WC (≤0.5 μm, >99.9%, Taegutec Ltd.), and Ni (≤10.0 μm, >99.5%, Yuelong Metal Powder Ltd.) powders were used as the initial materials. These powders were synthesised via HEBM using WC balls at

<sup>1</sup> AUTOMOTIVE MATERIALS & COMPONENT R&D GROUP, KOREA INSTITUTE OF INDUSTRIAL TECHNOLOGY, 6, CHEOMDAN-GWAGIRO 208-GIL, BUK-GU, GWANGJU, 61012, KOREA

\* Corresponding author: [hk-park@kitech.re.kr](mailto:hk-park@kitech.re.kr)



a ball-to-powder ratio of 2:1. The nominal composition of the TiC-based powder was mechanically alloyed to TiC-15Mo<sub>2</sub>C-10WC-9.6Ni (TMWN) with ethanol at 300 rpm, wherein the milling time was 6, 12, 24, and 48 h. The milled powders were consolidated by SPS (SPS 9.40 MK-III, Sumitomo Heavy Industries) at a sintering temperature of 1300°C and a heating rate of 60°C/min under a pressure of 60 MPa using a pyrometer. In addition, the phase composition between start (500°C) and completion (1300°C) of the shrinkage behaviour was compared. The microscopic shrinkage strain with the sintering kinetics was described by a generic equation (Eq. (1)).

$$\varepsilon^m = \left( \frac{\Delta l}{l_0} \right)^m = \frac{Kt}{T} \quad (1)$$

Where ‘*m*’ is the sintering exponent, *t* is the isothermal holding time and *T* is the hold temperature. The relative density of the sintered bodies was measured using Archimedes’ principle. The structural evolution of the TMWN cermet was examined by the X-ray diffraction with CuK $\alpha$  radiation ( $\lambda = 0.154$  nm). The average grain size of the TMWN cermet was obtained using the Image-Pro software from the FE-SEM images by measuring the length of the linear intercept. The microstructures of the TMWN cermet were observed via SEM, and their mechanical properties were measured using a Vickers hardness tester with a load of 20 kg·f applied for 15 s. The hardness was calculated using Eq. (2):

$$H_v = \frac{kP}{d^2} \quad (2)$$

Where *k* is a constant ( $k = 1.89 \times 10^5$ ) depending on the indenter geometry and units, *P* is the applied force (in N), and *d* is the

diagonal length of the indentation. In addition, the fracture toughness (*K<sub>IC</sub>*) value obtained using the Antis formula [4].

### 3. Results and discussion

Fig. 1 shows the densification profile of the TMWN cermet in terms of the densification strain and shrinkage rate during sintering for different HEBM times. The relative densities of all the samples were measured to be above 97.8% using Archimedes method (see TABLE 1). The shrinkage behaviour depended on the milling times. The significant shrinkage rates from low temperature (>200°C) lead to large agglomerates for the potential Kirkendall effect, the particles (or grains) in more grain boundary regions for neck formation were preferred during the solid-state sintering [5]. Moreover, the sintering exponent is related to densification stage with within the particle of strains during positive shrinkage section. According to Eq. (1), the lower the value of ‘*m*’, the higher is the magnitude of shrinkage. Therefore, the TMWN (48h milled) with the lowest ‘*m*’ value (1.29) showed high densification strain, which was believed to be due to the highly active diffusion routes at the lattice and grain boundaries throughout densification stage.

Fig. 2 shows the XRD patterns of the TMWN cermet at 500°C (Fig. 2a) and 1300°C (Fig. 2b). The most significant change in the phase constitution from the powder to the sintered body was noted from the solid solution to the core-rim structure according to the milling time, that is, from TiC+(Ti, W)C<sub>x</sub>+(Ti, Mo)C<sub>y</sub> (powder) to TiC+(Ti, W)C<sub>2</sub>+(Ti, Mo)C<sub>2</sub> (sintered body). The relative peaks of the TMWN cermet decreased with further milling, as shown in Figs. 2a and 2b. From the milling condi-

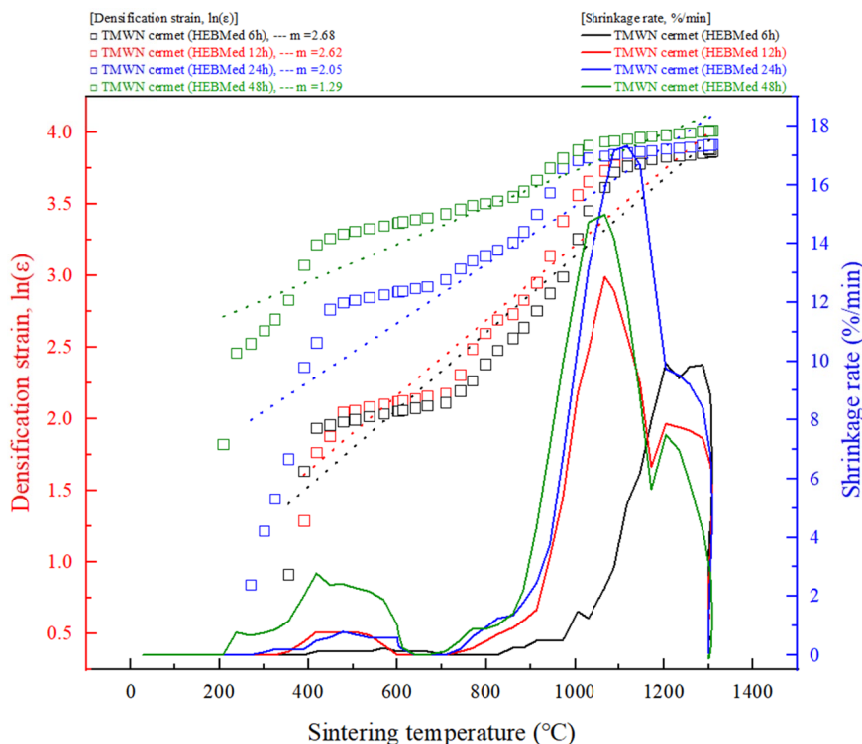


Fig. 1. Densification strain and shrinkage rate as a function of sintering temperature of TMWN cermet

TABLE 1

Details for lattice parameters and physical/mechanical properties of TMWN cermets

Specimen	Lattice parameter (Å), (2 Theta)		Micro strain (%)		Relative density (%)	Grain size ( $\mu\text{m}$ )	Standard deviation	Hardness (HV <sub>20</sub> , GPa)	Fracture toughness ( $K_{IC}$ , MPa·m <sup>1/2</sup> )
	500°C	1300°C	500°C	1300°C					
TMWN (HEBMed 6 h)	2.1364 (42.30°)	2.1539 (41.94°)	0.15	0.09	97.8	2.57	0.54	12.1±0.2	11.1±0.5
TMWN (HEBMed 12 h)	2.1410 (42.21°)	2.1554 (41.91°)	0.34	0.18	98.5	1.68	0.43	13.2±0.1	11.8±0.5
TMWN (HEBMed 24 h)	2.1431 (42.16°)	2.1560 (41.90°)	0.46	0.12	98.7	0.73	0.12	15.7±0.1	13.5±0.5
TMWN (HEBMed 48 h)	2.1433 (42.12°)	2.1566 (42.03°)	0.58	0.08	99.2	0.47	0.32	17.1±0.2	14.8±0.4

tions after 24 h, the W and Mo atoms agglutinated or embedded in the Ti matrix of the (111) and (200) planes more easily than maintaining the Ti-C bonds [6]; this facilitated short-range diffusion paths by the processes of fracturing and refinement

because of the precipitates of brittle intermetallics. It was found that the lattice parameters gradually increased (see TABLE 1) with further milling and high sintering temperatures, because of the accelerated dissolution of the W and Mo atoms into the TiC lattice owing to a decrease in grain (crystallite) sizes. In addition, the strain energy induced in the grain boundaries during the early sintering stage (~500°C) increased (0.15 to 0.58) upon further milling, which could lead to the formation of a solid solution such as (Ti, W)C<sub>x</sub> and (Ti, Mo)C<sub>y</sub>.

Fig. 3 shows the microstructure of the TMWN cermets obtained with different HEBM times. The TMWN cermets comprised a TiC core (black), M<sub>x</sub>C rims (white), and the Ni binder (grey). As the HEBM time was increased from 6 h (see Fig. 3a) to 12 h (see Fig. 3b), two types of core-rim structures were clearly observed between the Ni-binder regions: one with a fine core and the other with a coarse core. However, from 24 h to 48 h, there was no obvious distinction as the TiC-core became finer between the fine core-rim and Ni-binder phases. This tendency was attributed to the ‘solution-reprecipitation’ process dominating the ‘solid-diffusion’ between the fine particles and metallic binder during the rapid sintering process. Yanada et al. reported [7] that fine precipitates in the form of (Ti, W)C<sub>2</sub> and (Ti, Mo)C<sub>2</sub> were generated on each TiC grain, and the width of the rim structure increased because of the reprecipitation of the solutes. Consequently, it was assumed that the refinement of TiC promoted the formation of the core-rim structure. In fact, the average grain size of the TiC core decreased with further milling from 2.57 to 0.47  $\mu\text{m}$ . Fig. 3(e) shows the crack propagation of the TMWN cermet (48 h) with element mapping. The derived crack deflection occurred in the rim-rich regions surrounding the refined TiC-core (48 h milled) while resisting crack propagation, contrary to the crack extended directly through the large cores (6 h milled). This effect was attributed to the increased fracture toughness, which is an effective mediator of transgranular fractures. Owing to the continuous core-rim of W and Mo in the hard phase (TiC-core), the inner and outer rims would become thicker, leading to improved plasticity with a slip at the FCC structure (rim) to plastic deformation. If the Hall-Patch formula is applied to the grain refinement of the core according to severe mechanical milling, the cermet with ultrafine possess would enhance mechanical properties such as hardness and toughness. Therefore, it was considered that a rim structure during the sintering process

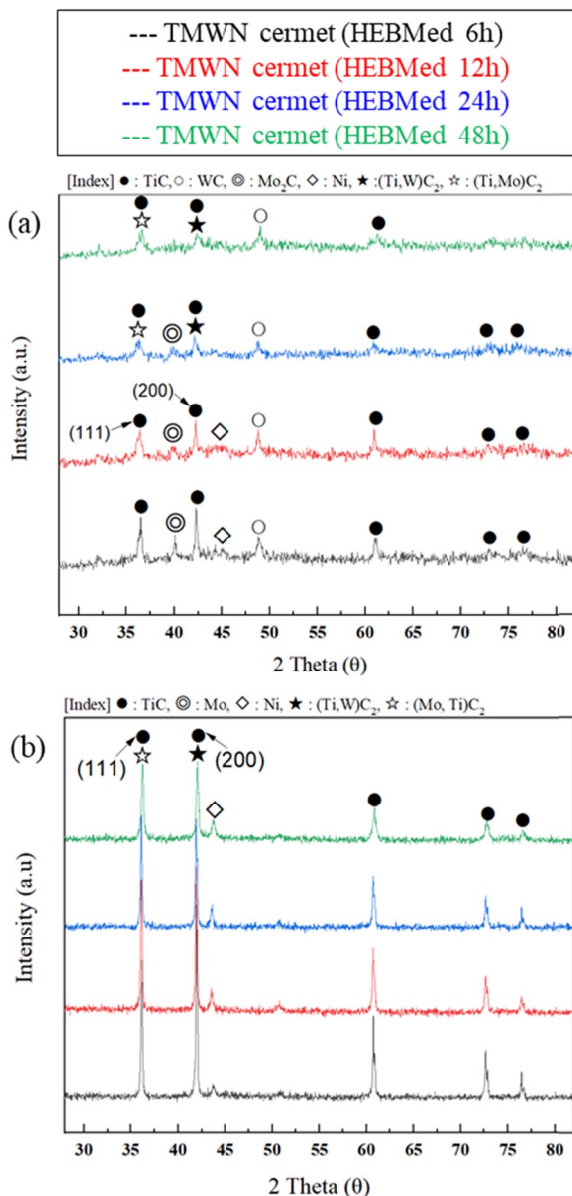


Fig. 2. XRD patterns of TMWN cermets as a function of sintering temperature: (a) 500°C and (b) 1300°C

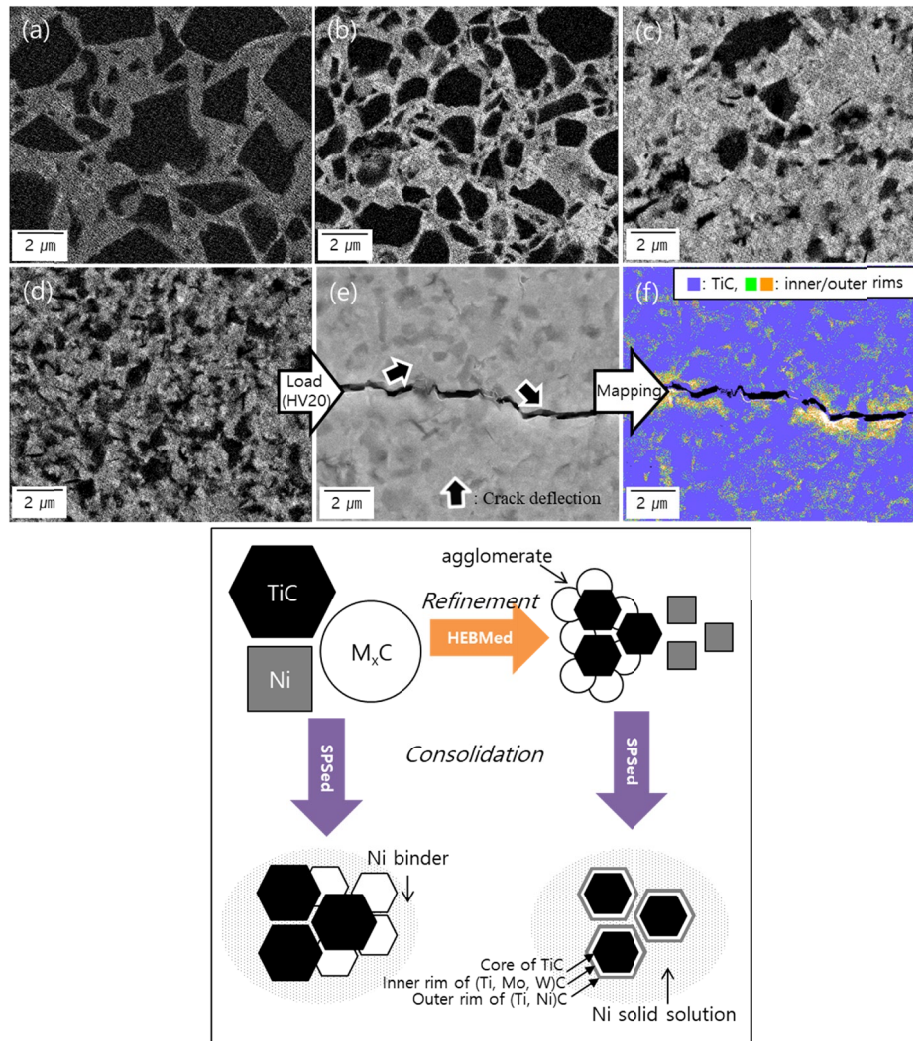


Fig. 3. FE-SEM images (BSED) and schematic representation of TMWN cermets in accordance with the HEBMed milling time: (a) 6h, (b) 12h, (c) 24h, (d) 48h, (e) crack propagation (48h), and (f) mapping, i.e. TiC-core (black), rims of  $M_xC$  (white), and Ni-binder (gray)

with a high fraction was formed on further milling; the toughness strengthening from  $11.1$  to  $14.8 \text{ MPa} \cdot \text{m}^{1/2}$  was mutually effective with grain boundary strengthening for the TiC-core.

#### 4. Conclusions

- 1) The TMWN cermet powder, to which continuous milling energy was applied, was advantageous for the neck formation because of the high specific surface area of the grain boundaries during the sintering process, thereby leading to a high relative density.
- 2) The phase composition of the TMWN cermets was significantly affected by the state of the pre-milled powder, and a gradual increase in the lattice parameter and strain energy was observed in the solid-solution formation during the densification process.
- 3) The mechanical properties of the TMWN cermets were characterised by considering the grain size and crack propagation with the core-rim structure, wherein the toughening effect was confirmed as the milling time increased.

#### Acknowledgments

This study has been conducted with support of the Korea Institute of Industrial Technology, Production Industry Leading Core Technology Development Project as the “Development of an on-site facility attached cryogenic machining integrated system (KITECH-EH-22-0093)”.

#### REFERENCES

- [1] J.H. Lee, I.H. Oh, H.K. Park, Arch. Metall. Mater. **66** (4), 1029-1032 (2021).
- [2] Z. Fu, R. Koc, Mater. Sci. Eng. A **676**, 278-288 (2016).
- [3] H.O. Andren, Mater. Chem. Phys. **67**, 209-213 (2001).
- [4] G.R. Antis, P. Chantikul, B.R. Lawn, D.B. Marshall, J. Am. Ceram. Soc. **64** (9), 533-538 (1981).
- [5] A. Ozer, O.B. Kilic, Acta Phys. Pol. A **131** (3), 329-331 (2017).
- [6] P. Li, J. Ye, Y. Liu, D. Yang, H. Yu, Int. J. Refract. Met. Hard Mater. **35**, 27-31 (2012).
- [7] Y. Yanaba, T. Takahashi, K. Hayashi, J. Jpn. Soc. Powder Metallurgy **51** (5), 374-384 (2004).